



Published in final edited form as:

Traffic. 2020 July ; 21(7): 503–517. doi:10.1111/tra.12736.

Phosphatidylinositol 3,5-bisphosphate regulates Ca²⁺ transport during yeast vacuolar fusion through the Ca²⁺ ATPase Pmc1

Gregory E. Miner¹, Katherine D. Sullivan¹, Chi Zhang¹, David Rivera-Kohr¹, Annie Guo¹, Logan R. Hurst¹, Ez C. Ellis¹, Matthew L. Starr¹, Brandon C. Jones¹, Rutilio A. Fratti^{1,2}

¹Department of Biochemistry, University of Illinois at Urbana-Champaign, Urbana, Illinois

²Center for Biophysics and Quantitative Biology, University of Illinois at Urbana-Champaign, Urbana, Illinois

Abstract

The transport of Ca²⁺ across membranes precedes the fusion and fission of various lipid bilayers. Yeast vacuoles under hyperosmotic stress become fragmented through fission events that requires the release of Ca²⁺ stores through the TRP channel Yvc1. This requires the phosphorylation of phosphatidylinositol-3-phosphate (PI3P) by the PI3P-5-kinase Fab1 to produce transient PI(3,5)P₂ pools. Ca²⁺ is also released during vacuole fusion upon *trans*-SNARE complex assembly, however, its role remains unclear. The effect of PI(3,5)P₂ on Ca²⁺ flux during fusion was independent of Yvc1. Here, we show that while low levels of PI(3,5)P₂ were required for Ca²⁺ uptake into the vacuole, increased concentrations abolished Ca²⁺ efflux. This was as shown by the addition of exogenous dioctanoyl PI(3,5)P₂ or increased endogenous production of by the hyperactive *fab1^{T2250A}* mutant. In contrast, the lack of PI(3,5)P₂ on vacuoles from the kinase dead *fab1^{EEE}* mutant showed delayed and decreased Ca²⁺ uptake. The effects of PI(3,5)P₂ were linked to the Ca²⁺ pump Pmc1, as its deletion rendered vacuoles resistant to the effects of excess PI(3,5)P₂. Experiments with Verapamil inhibited Ca²⁺ uptake when added at the start of the assay, while adding it after Ca²⁺ had been taken up resulted in the rapid expulsion of Ca²⁺. Vacuoles lacking both Pmc1 and the H⁺/Ca²⁺ exchanger Vcx1 lacked the ability to take up Ca²⁺ and instead expelled it upon the addition of ATP. Together these data suggest that a balance of efflux and uptake compete during the fusion pathway and that the levels of PI(3,5)P₂ can modulate which path predominates.

Keywords

Fab1; Fig4; PIKfyve; Pmc1; Vcx1; Yvc1

Correspondence Rutilio A. Fratti, Department of Biochemistry, University of Illinois at Urbana-Champaign, 417 Roger Adams Laboratory, B-4, 600 S. Mathews Ave. Urbana, IL 61801. rfratti@illinois.edu.
Gregory E. Miner and Katherine D. Sullivan contributed equally to this study.

AUTHOR CONTRIBUTIONS

GEM, KDS, CZ, DAR-K and RAF, Conception and design, Data analysis and interpretation, Drafting or revising the article; GEM, KDS, AG, CZ, DAR-K, MLS, ECE and BCJ Acquisition of data, data analysis.

CONFLICT OF INTEREST

The authors declare that they do not have conflicts of interest with the contents of this article.

1 | INTRODUCTION

The role of Ca^{2+} as a regulator of membrane fusion is best understood in the release of neurotransmitters through the fusion of synaptic vesicles with the presynaptic plasma membrane.¹ Upon plasma membrane depolarization an influx of Ca^{2+} into the cytoplasm occurs which subsequently binds to the C2 domains of synaptotagmin-1. Once bound to Ca^{2+} , synaptotagmin-1 changes conformation and aids in triggering SNARE-mediated fusion.² Ca^{2+} transport across membranes is also a part of endolysosomal trafficking. In *Saccharomyces cerevisiae* vacuolar lysosomes serve as the major Ca^{2+} reservoir where it is complexed with inorganic polyphosphate.³ The transport of Ca^{2+} into the vacuole lumen is mediated through the $\text{Ca}^{2+}/\text{H}^{+}$ exchanger Vcx1, and the Ca^{2+} ATPase pump Pmc1, whereas the movement out of the lumen into the cytoplasm is performed by the Ca^{2+} channel Yvc1, a mucolipin transient receptor potential cation channel (TRPML) family orthologue.⁴

To date, we have a partial understanding of the mechanisms driving the release of Ca^{2+} during intracellular membrane trafficking. During osmotic shock or mechanical stress Yvc1 transports Ca^{2+} from the vacuole lumen to the cytosol in a manner that is controlled in part by the formation of $\text{PI}(3,5)\text{P}_2$ by the PI3P 5-kinase Fab1/PIKfyve.⁵⁻⁸ Through uncertain mechanisms this cascade leads to the fragmentation of the vacuole into small vesicles through fission events.

During membrane fusion the release of Ca^{2+} is triggered by *trans*-SNARE pairing.⁹ However, a role for $\text{PI}(3,5)\text{P}_2$ for fusion related Ca^{2+} efflux has not been tested. Previously, we showed that vacuole fusion was inhibited in the presence of elevated $\text{PI}(3,5)\text{P}_2$.¹⁰ Fusion was blocked by either the addition of an exogenous dioctanoyl form of the lipid (C8- $\text{PI}(3,5)\text{P}_2$) or through endogenous overproduction by the hyperactive *fab1*^{T2250A} mutant. Fusion was arrested after the formation of *trans*-SNARE pairs but before mixing of the outer leaflets, that is, hemifusion. The possible role for the TRP Ca^{2+} channel Yvc1 in the inhibition of fusion by $\text{PI}(3,5)\text{P}_2$ was eliminated, as vacuoles lacking the transporter fused well and were equally sensitive to $\text{PI}(3,5)\text{P}_2$ relative to wild type vacuoles. Although Yvc1 was not involved in the arrest of fusion, others have shown that Ca^{2+} efflux still occurs in the absence of the channel.⁹ Thus, we postulated that $\text{PI}(3,5)\text{P}_2$ could affect Ca^{2+} transport through a separate mechanism.

Various mechanisms control the involvement of Ca^{2+} transport in membrane fusion including Ca^{2+} -binding protein calmodulin and a specific ABC transporter. Calmodulin acts as a sensor and participates in triggering late fusion events. Calmodulin tightly binding vacuoles upon Ca^{2+} release signals the completion of docking, which stimulates bilayer mixing.^{11,12} Another mechanism that regulates fusion events through modulating Ca^{2+} transport involves the vacuolar Class-C ABC transporters Ybt1.^{13,14}

Here we continued our study of $\text{PI}(3,5)\text{P}_2$ during fusion and found that elevated concentrations of the lipid blocked the release of Ca^{2+} . Both exogenous C8- $\text{PI}(3,5)\text{P}_2$ and overproduction by *fab1*^{T2250A} inhibited Ca^{2+} efflux. In contrast, Ca^{2+} efflux was enhanced when Fab1 was inhibited by Apilimod, or when $\text{PI}(3,5)\text{P}_2$ was sequestered by ML1-N. This

effect was reproduced by the kinase dead *fab1^{EEE}* mutation. Finally, we found that the effect of PI(3,5)P₂ on Ca²⁺ transport depends on the Ca²⁺ uptake pump Pmc1 and not Yvc1.

2 | RESULTS

2.1 | Ca²⁺ efflux is inhibited by PI(3,5)P₂

The release of vacuole luminal Ca²⁺ stores occurs upon *trans*-SNARE complex formation in the path towards fusion.⁹ The formation of vacuolar SNARE complexes also relies on the assembly of membrane microdomains enriched in regulatory lipids that include phosphoinositides such as the Fab1 substrate PI3P.¹⁵ However, the link between phosphoinositides and Ca²⁺ transport during fusion has remained unclear. By contrast, the dependence of Ca²⁺ efflux on PI(3,5)P₂ during vacuole fission under hyperosmotic conditions has been established.⁷ Together, this served as the impetus to explore the role of PI(3,5)P₂ in fusion-linked Ca²⁺ transport.

To address this gap in knowledge, we used isolated vacuoles for in vitro assays of Ca²⁺ flux. Ca²⁺ transport was monitored through changes in Fluo-4 (or Cal-520) fluorescence as previously demonstrated.^{13,16-18} Vacuoles were incubated under fusion conditions and reactions were started by the addition of ATP. As seen before, the addition of ATP triggers the rapid uptake of extraluminal Ca²⁺ from the buffer into the vacuole lumen as shown by the decrease in fluorescence (Figure 1A, black line). Omission of ATP prevented Ca²⁺ uptake and fluorescence remained flat (not shown). Shortly after, and in a SNARE-dependent manner, Ca²⁺ was released from vacuoles as shown by an increase in fluorescence. As a negative control for SNARE-dependent efflux, select reactions were incubated with antibody against Sec17 (α -SNAP), a co-chaperone of Sec18 (NSF) that aids in disrupting inactive *cis*-SNARE complexes to initiate the fusion pathway (Figure 1A, dotted line).¹⁹

Here, we tested the effects of PI(3,5)P₂ on Ca²⁺ transport. We incubated reactions with dioctanoyl (C8) derivatives of PI(3,5)P₂, PI3P and phosphatidic acid (PA). PA was included due to its inhibitory effect on vacuole fusion through the inhibition of *cis*-SNARE priming,²⁰ while PI3P was included as a precursor to PI(3,5)P₂ and as a pro-fusion lipid.^{16,21-24} Short chain lipids were used to avoid solubility issues. As a result, seemingly high concentrations of C8 lipids were needed to see an effect. This, however, does not reflect the mol% of the lipids that partition into the membrane bilayer. Collins and Gordon showed that only a small fraction of C8-lipids incorporate into the membrane.²⁵ Based on their work we estimated that 100 μ M C8-PI(3,5)P₂ correlated to ~1 mol% partitioned to the membrane fraction, which was in keeping with what reconstituted proteoliposome studies use in fusion models.²⁶ Lipids were added after Ca²⁺ uptake plateaus (arrows). We found that C8-PI(3,5)P₂ blocked Ca²⁺ efflux in a dose dependent manner and as effectively as the anti-Sec17 IgG negative control (Figure 1A,D, red lines). In parallel we found that C8-PI3P only showed a modest inhibition at the highest concentration tested when compared to C8-PI(3,5)P₂ (Figure 1B,D). When C8-PA was tested we found that it had no effect on Ca²⁺ efflux (Figure 1C,D). These data indicated that the Ca²⁺ efflux associated with vacuole fusion was blocked by PI(3,5)P₂. This is in contrast to the stimulatory effect of PI(3,5)P₂ on Ca²⁺ efflux associated with vacuole fission. Importantly the concentrations used do not fully

inhibit fusion, suggesting that Ca^{2+} transport can be uncoupled from fusion by altering the lipid composition of vacuole.¹⁰

2.2 | Inhibition of the PI3P 5-kinase Fab1 leads to enhanced Ca^{2+} efflux

To verify the effect of $\text{PI}(3,5)\text{P}_2$ on Ca^{2+} efflux we sought to counter its effects through inhibiting its production. The small molecule Apilimod had been shown to inhibit mammalian PIKfyve.^{27,28} Thus, we first tested if Apilimod could inhibit yeast Fab1 activity. For this we measured the conversion of BODIPY-TMR C6-PI3P to BODIPY-TMR C6- $\text{PI}(3,5)\text{P}_2$ by isolated vacuoles. Before we tested the effects of Apilimod, we verified our detection system by using *fig4* and *fab1* vacuoles that reduce or abolish $\text{PI}(3,5)\text{P}_2$ production, respectively. Using thin layer chromatography, we found that wild type vacuoles phosphorylated BODIPY-TMR C6-PI3P to make BODIPY-TMR C6- $\text{PI}(3,5)\text{P}_2$ (Figure 2A,B). The half-life of the product was observed to be short as the levels of BODIPY-TMR C6- $\text{PI}(3,5)\text{P}_2$ was significantly reduced after 5 minutes of incubation. This was in keeping reports by others showing that $\text{PI}(3,5)\text{P}_2$ has a short half-life during vacuole fission.²⁹⁻³¹ Next, vacuoles were incubated in the presence of BODIPY-TMR C6-PI3P and incubated with either vehicle or Apilimod to inhibit Fab1 activity. Indeed, Apilimod treatment abolished BODIPY-TMR C6- $\text{PI}(3,5)\text{P}_2$ generation (Figure 2C,D). It should be noted that high concentrations of Apilimod were needed to inhibit $\text{PI}(3,5)\text{P}_2$ production relative to the nM IC_{50} of Apilimod for mammalian PIKfyve.²⁷ The high concentrations needed here are probably due to the high dissociation rates of the molecule to the active site of yeast Fab1. This is often seen when inhibitors of mammalian orthologs are used with yeast where the effective dose can differ by orders of magnitude. This is exemplified by the effects of propranolol on inhibiting PA phosphatase activity on mammalian Lipin1 (μM) vs yeast Pah1 (mM),^{32,33} Latrunculin-B on actin polymerization (nM vs μM),^{34,35} and the PI 3-kinase inhibitor wortmannin (nM vs μM).^{21,36}

To visualize the effect of Apilimod on intact vacuoles we performed docking assays where endogenously produced $\text{PI}(3,5)\text{P}_2$ was labeled with Cy3-ML1-N as described previously.¹⁰ ML1-N is the N-terminal polypeptide from the endolysosomal mucopolin transient receptor potential (TRPML) Ca^{2+} channel.⁷ ML1-N preferentially binds to $\text{PI}(3,5)\text{P}_2$ on isolated yeast vacuoles as no labeling is observed with vacuoles from the kinase inactive *fab1^{EEE}* mutant.¹⁰ In Figure 2E, we show that vacuoles incubated with carrier (DMSO) showed distinct $\text{PI}(3,5)\text{P}_2$ punctate staining as previously reported. When vacuoles were incubated with Apilimod, we found that Cy3-ML1-N puncta were eliminated, further illustrating that Fab1 activity was inhibited during the experiment. Some free dye accumulated in the vacuole lumen to give the background fluorescence.

2.3 | Apilimod alters Ca^{2+} transport

The effects of Apilimod were next tested on Ca^{2+} efflux. First, we added a concentration range of Apilimod, or DMSO (carrier) at the beginning of the assay. This showed that Ca^{2+} uptake was inhibited by Apilimod in a dose dependent manner (Figure 3A,B). This suggested that some Fab1 activity was needed at the beginning of the reaction to allow Ca^{2+} transport into the vacuole lumen. In parallel, we tested whether acute inhibition of $\text{PI}(3,5)\text{P}_2$ production would have an effect on vacuole fusion. In Figure 3B, we show that

vacuole fusion was not significantly affected by Apilimod, indicating that newly synthesized PI(3,5)P₂ was not necessary for fusion to occur. Importantly, it also indicated that Apilimod did not have broad non-specific effects on the fusion machinery. We tested Apilimod after Ca²⁺ was taken up by vacuoles to examine its effects on efflux. The addition of Apilimod enhanced the release of Ca²⁺ in a dose dependent manner (Figure 3C,D). This suggested that blocking PI(3,5)P₂ production promoted Ca²⁺ efflux, which complimented the inhibition of Ca²⁺ release through the addition of C8-PI(3,5)P₂ shown in Figure 1. The DMSO carrier control had no effect as shown by the overlapping curve with buffer control. It is important to note that pre-existing PI(3,5)P₂ remained on the vacuole upon Apilimod treatment. To compare the effects of new lipid production with the starting pool of PI(3,5)P₂ we tested whether physically blocking PI(3,5)P₂ with ML1-N would reproduce the effects seen with Apilimod. When ML1-N was added we found that efflux was increased, which partially reproduced the Apilimod affect (Figure 3E,F). However, higher concentrations (1 μM) started to reduce efflux. Unlike Apilimod, high levels of ML1-N was expected to sequester any unbound PI(3,5)P₂. This was in agreement with the notion that low levels of PI(3,5)P₂ are needed for the fusion pathway to progress, while its absence or excess have deleterious effects on the system.¹⁰

2.4 | Fab1 kinase activity mutants differentially affect Ca²⁺ transport

Thus far we have used exogenous C8-PI(3,5)P₂, chemical inhibition of Fab1, and lipid sequestration to show that Ca²⁺ efflux is affected by this lipid. To further confirm these findings, we next used vacuoles from yeast that expressed Fab1 mutations that altered kinase activity. First, we used vacuoles that contained the hyperactive Fab1 kinase mutation T2250A.³⁷ We found that *fab1*^{T2250A} vacuoles showed blocked Ca²⁺ release early in the assay when wild type vacuoles showed peak release at ~15 minutes (Figure 4A, red). This was followed by delayed release by *fab1*^{T2250A} vacuoles that eventually reached wild type levels only after 60 minutes of incubation. We propose that the delay in Ca²⁺ release by *fab1*^{T2250A} vacuoles could be due to an increased time required for phosphatase Fig4 to reduce the levels of PI(3,5)P₂ present on these organelles. This was in keeping with the effects of adding exogenous C8-PI(3,5)P₂ in Figure 1A and supports the idea that elevated PI(3,5)P₂ concentrations suppress Ca²⁺ efflux. The delay in efflux seen with low concentrations of C8-PI(3,5)P₂ was close to what we observed with *fab1*^{T2250A} vacuoles and suggests that the prolonged inhibition by higher lipid concentrations was due to overwhelming the capacity of Fig4 to act on PI(3,5)P₂ in the duration of the experiment. To verify that the decreased Ca²⁺ efflux seen with *fab1*^{T2250A} vacuoles was due to directly to changes in PI(3,5)P₂ concentrations, we added Apilimod to block PI(3,5)P₂ synthesis. We found that blocking Fab1 activity restored Ca²⁺ release from *fab1*^{T2250A} vacuoles at low concentrations, while at higher concentrations led to enhanced efflux relative to wild type vacuoles (Figure 4B). The data points reflect the normalized levels of fluorescence after 30 minutes of incubation. In parallel we found that sequestering “excess” lipid with ML1-N also restored Ca²⁺ efflux *fab1*^{T2250A} vacuoles to wild type levels (Figure 4C). ML1-N at concentrations at or above 500 nM reduced Ca²⁺ as seen in Figure 3. Although the rescue was not as pronounced as the effect of Apilimod, the trend is consistent with the notion that elevated PI(3,5)P₂ reduces Ca²⁺ efflux.

To better our sense of how PI(3,5)P₂ concentrations serve as a switch to affect Ca²⁺ transport, we next used vacuoles from yeast that expressed the kinase-dead *fab1^{EEE}* mutation.³⁸ In Figure 4D, we show that *fab1^{EEE}* showed a delay and overall reduction in Ca²⁺ uptake compared to wild type. The eventual release of Ca²⁺ was also delayed, yet sizeable. Together the altered uptake and release of Ca²⁺ by *fab1^{EEE}* vacuoles reproduced the effects of adding Apilimod alone. The delay itself could be attributed to the reduced level of Sec17 present on *fab1^{EEE}* vacuoles.¹⁰ While priming was not tested it remains possible that a reduction in Sec17 would delay the critical amount of *trans*-SNARE pairing to trigger Ca²⁺ release earlier during the incubation to match the other assays.

To see if the effects of *fab1^{EEE}* were due to the lack of PI(3,5)P₂, we added exogenous C8-PI(3,5)P₂ and found that the Ca²⁺ efflux of *fab1^{EEE}* vacuoles was shifted down to wild type levels (Figure 4E). In contrast, our previous work showed PI(3,5)P₂ was unable to restore the fusion defect of *fab1^{EEE}*, which we attributed to separate vacuolar sorting defects.¹⁰ This suggests that the regulation of Ca²⁺ efflux by PI(3,5)P₂ is distinct from its effects on protein sorting to the vacuole. Collectively with the effect of overproducing PI(3,5)P₂, these data demonstrate that PI(3,5)P₂ can serve as a rheostat to either inhibit or enhance Ca²⁺ release from vacuoles. Furthermore, the effects of PI(3,5)P₂ on Ca²⁺ release appear to be oppositely regulated during osmotic shock vs isotonic conditions, as elevated PI(3,5)P₂ induces Ca²⁺ efflux under hyperosmotic conditions.⁷

In parallel, we tested the effect of deleting the PI(3,5)P₂ 5-phosphatase *FIG4* on Ca²⁺ transport. Cells lacking Fig4 have reduced levels of PI(3,5)P₂ produced during osmotic shock,^{29,30} and, thus, we predicted that it would have an intermediate effect compared to vacuoles with the *fab1^{EEE}* mutation. As expected *fig4* vacuoles showed attenuated Ca²⁺ uptake similar to *fab1^{EEE}* yet did not show the same delays in Ca²⁺ uptake or efflux (Figure 4E). Due to the reduced level of PI(3,5)P₂ present on *fig4* vacuoles we expected that Ca²⁺ efflux would be resistant to added C8-PI(3,5)P₂. In accord with the other data, *fig4* vacuoles were indeed resistant to C8-PI(3,5)P₂ compared to wild type vacuoles (Figure 4F). This is consistent with our previous finding with *fig4* vacuoles and lipid mixing.¹⁰

2.5 | PI(3,5)P₂ affects Ca²⁺ transport in a Pmc1 dependent manner

To hone in on the mechanism by which PI(3,5)P₂ regulates Ca²⁺ flux during fusion we generated knockouts of the known vacuolar Ca²⁺ transporters: Pmc1, Vcx1, and Yvc1. As reported by Merz and Wickner, deletion of these transporters was unable to abolish the release of Ca²⁺ during fusion.⁹ In keeping with their findings, we found that Ca²⁺ efflux was close to wild type with each of the deletion strains (Figure 5A,B). We next asked if treating these deletion strains with C8-PI(3,5)P₂ would inhibit Ca²⁺ flux to the same extent as seen with wild type vacuoles. We found that C8-PI(3,5)P₂ inhibited Ca²⁺ efflux in vacuoles from *yvc1* and *vcx1* strains, but not those from *pmc1* yeast (Figure 5A,B). Thus, it was probably that PI(3,5)P₂ affected Ca²⁺ transport in a Pmc1-dependent manner. Because Pmc1 transports Ca²⁺ into the vacuole, the effect on the observed efflux could be due to the hyper-stimulation of Pmc1. It is important to emphasize that deleting *YVC1* had no effect on the inhibition of Ca²⁺ flux by PI(3,5)P₂. While Yvc1 is essential for the PI(3,5)P₂ activated Ca²⁺ transport during vacuole fission, this channel does not appear to play a role

during vacuole fusion, which is in keeping with our previous report.¹⁰ Others have suggested that leakage can occur during vacuole fusion when SNAREs are overexpressed.³⁹ Thus, it could be that a similar leakage could serve as a transient Ca²⁺ pore. However, the ability of PI(3,5)P₂ to inhibit net Ca²⁺ efflux at concentrations that do not inhibit fusion argues that the effects seen here are not due to non-specific leakage.

If PI(3,5)P₂ was truly acting to trigger Pmc1 activity we hypothesized that the effect could be reversible by the Ca²⁺ pump inhibitor Verapamil.^{40,41} While there are no report of Verapamil inhibiting Pmc1, the sarcoendoplasmic reticulum Ca²⁺ ATPase pump (SERCA) has been shown to be inhibited by Verapamil at 290 μM.⁴² In our experiments we found that Verapamil blocked the effect of C8-PI(3,5)P₂ on Ca²⁺ efflux (Figure 5B). This further indicates that the observed net Ca²⁺ efflux could instead be the inhibition of further Ca²⁺ uptake while the cation is released at a constant rate by another mechanism.

The effects of PI(3,5)P₂ on the different strains suggested that the net Ca²⁺ efflux observed during fusion is in fact due to a change in the balance between uptake and efflux. This would consistent with the effect of PI(3,5)P₂ Ca²⁺ flux in a Pmc1-dependent manner. To further examine this, we used vacuoles from *vcx1 pmc1* double deletion strains. The double deletion of these importers was expected to abolish Ca²⁺ uptake in the presence of ATP. In Figure 6A we show that in the absence of ATP, both wild type and *vcx1 pmc1* vacuoles were unable to take up Ca²⁺. Unexpectedly, upon the addition of ATP, *vcx1 pmc1* vacuoles immediately expelled Ca²⁺, the opposite of the uptake observed with wild type vacuoles. The levels of Ca²⁺ release by *vcx1 pmc1* vacuoles reached the maximum detection levels of the plate reader when set to detect to Ca²⁺ flux from both mutant and wild type vacuoles. Lowering the gain for *vcx1 pmc1* vacuoles would render wild type flux undetectable. The expulsion of Ca²⁺ by *vcx1 pmc1* vacuoles was resistant to anti-Sec17 IgG, indicating that the release was SNARE independent. We next tested if the efflux of Ca²⁺ by *vcx1 pmc1* vacuoles was sensitive to PI(3,5)P₂ and found that the addition of this lipid had no effect on Ca²⁺ release (Figure 6B,C). This suggests that the effects of PI(3,5)P₂ occur during the Ca²⁺ uptake phase. Based on these data we hypothesized that in the presence of ATP, vacuoles constitutively release Ca²⁺, and that its detection is normally overcome by the dual action of Vcx1 and Pmc1. The production of PI(3,5)P₂ early in the reaction promotes Ca²⁺ uptake in a Pmc1-dependent manner. The short half-life of the lipid could then reduce uptake, resulting in the in the observed Ca²⁺ efflux.

The yeast vacuole is predicted to only have Pmc1 and Vcx1 to import Ca²⁺. This was supported by the data above as deletion of both abolished vacuolar Ca²⁺ uptake. Thus, deleting *VCX1* alone would leave only Pmc1 on the vacuole, and results seen with *vcx1* vacuoles would serve as a reporter for Pmc1 activity. Based on this, we next tested the effect of adding Verapamil and Apilimod at the beginning of the assay to measure Ca²⁺ uptake with *vcx1* vacuoles. We observed that Ca²⁺ uptake was inhibited by both reagents, with Verapamil having a greater effect vs Apilimod (Figure 6D,E). These data were consistent with the hypothesis that Pmc1 mediated Ca²⁺ uptake is sensitive to PI(3,5)P₂ levels.

To additionally test the balance of Ca^{2+} uptake and release during the pathway, we further examined the effects of Verapamil. First, we showed that verapamil blocks Ca^{2+} uptake in a dose dependent manner and in the range seen to inhibit mammalian SERCA. Vacuoles incubated with a concentration range of Verapamil at the beginning of the assay. Using wild type vacuoles, we found that Verapamil inhibited Ca^{2+} uptake in a dose dependent manner when added at the beginning of the assay (Figure 7A,B). This had little effect on vacuole fusion. Next, we tested if Ca^{2+} uptake continues late in the reaction by adding Verapamil after the initial uptake of Ca^{2+} . As seen in Figure 7C, D, adding Verapamil after Ca^{2+} uptake resulted in a rapid accumulation of extraluminal Ca^{2+} . This suggests that under control conditions, Ca^{2+} uptake continues through the docking stage, 10 to 15 minutes into the pathway, after which uptake is either inactivated or simply overcome by Ca^{2+} efflux.

Given the surprising result that Ca^{2+} efflux appeared to be triggered by a reduction in Pmc1 activity we sought to clarify whether the main cause of Ca^{2+} efflux during membrane fusion was through the generation of transient pores as has been proposed. If transient pore formation serves as the primary efflux pathway, then we would only expect Verapamil to trigger Ca^{2+} efflux if fusion was allowed to proceed. We found that extraluminal Ca^{2+} increased over the baseline in the presence of Verapamil and anti-Sec17 IgG, however, the amount detected was half of what was seen with Verapamil alone. This suggests that the increase in extraluminal Ca^{2+} seen with Verapamil was not due to pore formation.

2.6 | $\text{PI}(3,5)\text{P}_2$ and Pmc1 interactions with Nyv1 and the V-ATPase

Others have previously shown that Pmc1 activity is inhibited in part through its binding to the vacuolar R-SNARE Nyv1.⁴³ Separately, $\text{PI}(3,5)\text{P}_2$ has been shown to stabilize $V_0 - V_1$ holoenzyme assembly.³⁸ Further, Pmc1 physically interacts with the V-ATPase. Thus, we thought it important to examine if this lipid affected the interactions between these proteins to shed further light onto a novel mechanism that controls Ca^{2+} transport. To accomplish this, we used vacuoles that harbored Pmc1 tagged with the triple hemagglutinin (HA) epitope in order to perform co-immunoprecipitation (IP) assays.⁴⁴ Figure 8A shows that IP of wild type vacuoles anti-HA antibody did not pull down anything, ensuring that complexes pulled down from the Pmc1-HA3 strain would not be spurious. When Pmc1-HA3 vacuoles were used we observed a clear band corresponding to the tagged pump. IP of Pmc1-HA3 with anti-HA IgG isolated Pmc1-HA3 in addition to Nyv1 and Vph1, a component of the membrane integrated V_0 complex of the V-ATPase. Vph1 has been shown to bind Pmc1 in a high throughput screen of the yeast protein interactome.⁴⁵

Next, we examined Pmc1 interactions in the presence of buffer, C8- $\text{PI}(3,5)\text{P}_2$, ML1-N and Apilimod. We found that C8- $\text{PI}(3,5)\text{P}_2$ did not alter the interactions between Pmc1 and Nyv1. However, blocking $\text{PI}(3,5)\text{P}_2$ production with Apilimod partially reduced the amount of Nyv1 that co-immunoprecipitated with Pmc1 (Figure 8B,C). Although, $\text{PI}(3,5)\text{P}_2$ is not known to bind either Nyv1 or Pmc1 directly, it has been shown to bind to the V_0 component Vph1 where it stabilizes $V_0 - V_1$ holoenzyme assembly.³⁸ Because the V-ATPase is known to bind Pmc1 we tested if C8- $\text{PI}(3,5)\text{P}_2$ would affect Pmc1-Vph1 interactions.⁴⁵ We found that $\text{PI}(3,5)\text{P}_2$ led to a partial reduction in Vph1 interactions with Pmc1. Although, these interactions were not completely abolished, it is still possible that function was altered with

minimal changes to the stoichiometry of the complex. Such a scenario has been documented with SNARE complexes on yeast vacuoles, where *trans*-SNARE complexes form, yet fail to induce vacuole fusion for various reasons.^{10,46} It is also possible that complex sub-units that remain to be identified could be affected more drastically by changes in PI(3,5)P₂. While it is not possible to conclusively say that PI(3,5)P₂ affects the Pmc1 protein complex, we can conclude that changes in PI(3,5)P₂ concentrations act as a controller affecting Ca²⁺ transport. Future studies will elucidate the relationship between the lipid and Ca²⁺ flux as well as how these effects could alter V-ATPase activity.

3 | DISCUSSION

The yeast vacuole serves as the primary reservoir for Ca²⁺ ions, which are translocated across the membrane through multiple transporters including Pmc1, Yvc1, and Vxc1. Although the regulatory mechanisms for each of these transporters are not fully understood, it has been shown that various lipids can affect their function in an organelle specific manner. For instance, PI(3,5)P₂ regulates Ca²⁺ release through Yvc1 during the osmotically driven vacuole fission.⁷ Ca²⁺ is also released from the vacuole during the fusion process upon the formation of *trans*-SNARE complexes.^{9,12,47} More recently, we found that elevated levels of PI(3,5)P₂ inhibits vacuole fusion at a stage between *trans*-SNARE pairing and outer-leaflet lipid mixing, that is, hemifusion and full bilayer fusion.¹⁰ This was observed through adding exogenous C8-PI(3,5)P₂ or through using *FAB1* mutations that were either kinase dead or overproduced the lipid. That study established that low levels of PI(3,5)P₂ are needed for fusion to occur, but elevated concentrations are inhibitory. At this point, it is unclear whether the effects of PI(3,5)P₂ are direct or if the ratio with its precursor PI3P and downstream degradation product(s) also play a role. In either circumstance, it is clear that PI(3,5)P₂ has a biphasic effect on vacuole fusion.

The biphasic nature of PI(3,5)P₂ in vacuole fusion is not limited to this lipid. For instance, PA is needed for reconstituted proteoliposome fusion to occur and for Vam7 binding to vacuoles.^{16,26} Yet, inhibiting PA phosphatase activity to produce diacylglycerol (DAG), resulting in elevating PA concentrations, blocks vacuole fusion at the priming stage through sequestering Sec18 from *cis*-SNARE complexes.^{20,48} Likewise, low levels of phospholipase C (PLC) stimulates vacuole fusion through converting PI(4,5)P₂ to DAG, while high levels of PLC potentially inhibits fusion.⁴⁹ Finally, while PI(4,5)P₂ is well known to stimulate vacuole fusion, an excess of the lipid can also inhibit the pathway.^{10,15,23,50} These examples show that the balance of substrate and product lipids can serve to move a pathway forward or arrest its progress.

In this study, we continued our investigation on the inhibitory nature of PI(3,5)P₂ on vacuole fusion. Our work has identified that elevated levels of PI(3,5)P₂ block the net Ca²⁺ efflux observed during fusion vacuole fusion. The effect of PI(3,5)P₂ on Ca²⁺ transport was shown by various means including the use of the kinase dead *fab1^{EEE}* and hyperactive *fab1^{T2250A}* mutants. While both mutants were previously shown to inhibit hemifusion,¹⁰ here we see that only *fab1^{T2250A}* inhibited Ca²⁺ efflux, which is in accord with a scenario in which excessive PI(3,5)P₂ is a negative regulator of the fusion pathway. In contrast, kinase dead *fab1^{EEE}* vacuoles attenuated Ca²⁺ uptake followed by a delayed release of the cation. In both

instances, Ca^{2+} flux was restored to near wild type levels when the amount of free $\text{PI}(3,5)\text{P}_2$ was increased on *fab1^{EEE}* vacuoles or reduced on *fab1^{T2250A}* vacuoles. The Ca^{2+} efflux seen with *fab1^{EEE}* vacuoles observed here, albeit delayed, combined with our previous report showing that hemifusion was inhibited by this mutant indicates that Ca^{2+} flux precedes hemifusion.

Another revelation that comes from these experiments is that the effect of $\text{PI}(3,5)\text{P}_2$ on Ca^{2+} transport was independent of the TRP channel Yvc1. This is contrary to what occurs during vacuole fission induced by osmotic stress, when $\text{PI}(3,5)\text{P}_2$ interacts with Yvc1 leading to the release of Ca^{2+} from the vacuole lumen.⁷ Our previous work with $\text{PI}(3,5)\text{P}_2$ suggested that this lipid inversely regulates fission and fusion. The current work further supports this model and specifies that the effects occur through differentially modulating Ca^{2+} transport across the vacuole bilayer. Surprisingly, we found that the inhibition of Ca^{2+} transport by $\text{PI}(3,5)\text{P}_2$ was dependent on the Ca^{2+} ATPase Pmc1, which utilizes ATP hydrolysis to move Ca^{2+} into the vacuole lumen against the concentration gradient. Furthermore, it appears that the effect on Ca^{2+} uptake is immediate, as treatment with the Fab1/PIKfyve inhibitor Apilimod led to a rapid release of Ca^{2+} , suggesting that $\text{PI}(3,5)\text{P}_2$ needs to be newly generated at low levels to regulate Ca^{2+} transport. Under unencumbered conditions it is probably that $\text{PI}(3,5)\text{P}_2$ levels are kept in check through the phosphatase activity of Fig4. One of the most striking findings from this study is that the Ca^{2+} efflux associated with fusion appears to be in part through the inactivation of Ca^{2+} influx. Additionally, our data suggests that the primary route of efflux can be uncoupled from membrane fusion as inhibition of SNARE priming was unable to prevent the trigger of Ca^{2+} efflux following treatment with Verapamil. We therefore conclude that there is a Ca^{2+} efflux route is opposed by Pmc1.

The regulation of Pmc1 on yeast vacuoles is unclear relative to other P-type Ca^{2+} ATPases. Notwithstanding, others have shown that the R-SNARE Nyv1 directly interacts with Pmc1 to reduce Ca^{2+} transport.⁴³ Although not directly shown, their model posits that increased Nyv1 would proportionally have increased interactions with Pmc1 to further reduce Ca^{2+} transport. We sought to learn if elevated $\text{PI}(3,5)\text{P}_2$ levels would dissociate the Nyv1-Pmc1 complex to derepress Ca^{2+} transport. In our hands, we found that the Nyv1-Pmc1 interaction was only reduced by ~25% when $\text{PI}(3,5)\text{P}_2$ production was inhibited by Apilimod. Alone, this makes it difficult to conclude whether the change was sufficient to directly cause the observed results. In parallel, adding C8- $\text{PI}(3,5)\text{P}_2$ reduced the amount of Vph1 that co-isolated with Pmc1. Together, these data are supportive of the idea that changes in $\text{PI}(3,5)\text{P}_2$ levels could affect complex assembly. This also suggests that changes in $\text{PI}(3,5)\text{P}_2$ levels could affect V-ATPase function. This is in accord with work from the Kane lab showing that $\text{PI}(3,5)\text{P}_2$ can alter $V_0 - V_1$ complex stability and the translocation of protons into the vacuole lumen.^{38,51}

Neither Pmc1, nor Nyv1 have been shown to bind $\text{PI}(3,5)\text{P}_2$ directly, which raises the question as to how this lipid could affect the complex? While a direct interaction has not been shown it is still possible that an indirect path exists. One of the few bona fide $\text{PI}(3,5)\text{P}_2$ binding proteins on the vacuole is the V_0 component Vph1.³⁸ Their work showed that $\text{PI}(3,5)\text{P}_2$ stabilized the assembly of the $V_1 - V_0$ holoenzyme. Because Vph1 binds Pmc1⁴⁵ and R-SNAREs have been shown to directly bind V_0 ,⁵² we hypothesized that

PI(3,5)P₂ could affect the results of Vph1-Pmc1 and Pmc1-Nyv1 interactions. Our Pmc1 immunoprecipitations showed that Vph1 indeed interacted with Pmc1 and that adding C8-PI(3,5)P₂ reduced the Pmc1 interaction with Vph1, though the reduction was moderate. When we consider that blocking V-ATPase activity results in a decrease in Ca²⁺ uptake by vacuoles,⁵³ we can venture to think that promoting V-ATPase activity through PI(3,5)P₂-Vph1 interactions and promotion of V₁ – V_O complex could inversely promote Ca²⁺ uptake by reducing Vph1-Pmc1 interactions. Our data taken together with the finding that blocking Vph1 activity anti-Vph1 antibody inhibits Ca²⁺ efflux⁴⁷ suggests Vph1 could bind and affect Pmc1, and that the addition of C8-PI(3,5)P₂ or anti-Vph1 might attenuate productive interactions. Thus, it is possible that PI(3,5)P₂ regulates Pmc1 in part through binding Vph1 and induce conformational change that alter the downstream outcomes of Pmc1-Vph1 interactions. Although this model is incomplete, we believe these data gives further insight into the mechanism behind Ca²⁺ efflux during the fusion process as well as the ability of PI(3,5)P₂ to act as a potent fusion-fission switch.

Our finding that PI(3,5)P₂ affects Pmc1 and not Yvc1 during fusion presents an apparent paradox with what is known about this lipid during fission. The dual role of PI(3,5)P₂ in fission and fusion is indeed complex and this study goes to further our understanding of the difference. During fission, Fab1 is activated leading to a spike of PI(3,5)P₂ on the vacuole. This activates the mechanosensitive TRP channel Yvc1 and efflux of luminal Ca²⁺ stores into the cytosol.⁷ During fusion, Fab1 is active and elevated levels of PI(3,5)P₂ inhibits fusion. In this paper, we show that one of the effects of elevated PI(3,5)P₂ is that the Ca²⁺ efflux associated with *trans*-SNARE complex formation is blocked. In order to tease these mechanisms apart we have to take into consideration the post-translational modification of Yvc1. During osmotic shock, 6 of the 9 surface exposed Cys on Yvc1 are modified with glutathione by Gtt1.^{54,55} After recovering from shock the attached glutathiones are removed by the thioreductase Trx2. Mutation of key Cys residues to Ser, or deletion of *GTT1* to prevent the addition of glutathione blocks Yvc1 from transporting Ca²⁺. Another consideration is that Yvc1 exists as a multimer in isotonic conditions as shown in large-scale proteomic studies.^{45,56} We propose that Gtt1 activity interferes with Yvc1 dimers to allow activation by PI(3,5)P₂ and promote Ca²⁺ flux. Taken together, we theorize that under isotonic conditions Yvc1 is not modified and the dimer is inactive. Further, Yvc1 is probably unable to interact with PI(3,5)P₂ in a manner that promotes Ca²⁺ transport. This is probably due to changes in affinity or steric hindrance by the unmodified Yvc1 dimer.

The spike in PI(3,5)P₂ production during osmotic shock not only activates Yvc1, but also stimulates V-ATPase activity.⁵⁷ The latter is probably due to the stabilization of the V₁ – V_O complexes.³⁸ As a result, the vacuole becomes more acidic and Ca²⁺ is released from the vacuole during fission. Under isotonic conditions, the lower levels of PI(3,5)P₂ present may be enough to activate V-ATPase activity, but not to overly acidify the vacuole. Thus, another important facet of PI(3,5)P₂ activity is the regulation of vacuolar acidification. In conclusion, this work adds to the body of evidence showing that PI(3,5)P₂ has multiple roles in vacuole dynamics including the switch between fusion and fission and the transport of Ca²⁺ and H⁺ across the membrane.

4 | MATERIALS AND METHODS

4.1 | Reagents

Soluble reagents were dissolved in PIPES-Sorbitol (PS) buffer (20 mM PIPES-KOH, pH 6.8, 200 mM sorbitol) with 125 mM KCl unless indicated otherwise. Anti-Sec17 IgG,¹⁹ and Pbi2⁵⁸ were prepared as described previously. C8-PA (1,2-dioctanoyl-*sn*-glycero-3-phosphate), C8-PI3P (1,2-dioctanoyl-phosphatidylinositol 3-phosphate), and C8-PI (3,5)P₂ (1,2-dioctanoyl-phosphatidylinositol 3,5-bisphosphate), BODIPY-TMR C6-PI3P and BODIPY-TMR C6-PI(3,5)P₂ were purchased from Echelon Inc. Apilimod was from MedKoo Biosciences and Verapamil was from Cayman Chemical. Both were dissolved in DMSO as stock solutions. Anti-HA antibody was from Thermo-Fisher. GST-ML1-N was produced as described.^{7,10} Cy3-maleimide (GE Healthcare) was used to label GST-ML1-N according to the manufacturer's instructions.

4.2 | Strains

Vacuoles from BJ3505 genetic backgrounds were used for Ca²⁺ flux assays (Table 1). *PMC1* was deleted by homologous recombination using PCR products amplified using 5'-PMC1-KO (5'-TTCTAAAAAATAAAACTGTGTGCGTAACAAAAAATAGACATGGAGGCCCA GAATAC-3') and 3'-PMC1-KO (5'-TTGGTCACTTACATTTGTATAAACATATAGAGCGCGTCTACAGTATAGCGACCAGCA TTC-3') primers with homology flanking the *PMC1* coding sequence. The PCR product was transformed into yeast by standard lithium acetate methods and plated on YPD media containing G418 (250 µg/µL) to generate BJ3505 *pmc1::kanMX6* (RFY84). Similarly, *VCX1* was deleted from BJ3505 by recombination using 5'-VCX1-KO (5'-TTCATCGGCTGCTGATAGCAAATAAAACAACATAGATACAGACATGGAGGCCCCAG AATAC-3') and 3'-VCX1-KO (5'-ATATAAAATTAGTTGCGTAAACATAATATGTATAATATACAGTATAGCGACCAGCAT TC-3') primers that flanked the *VCX1* open reading frame to make RFY86. The *vcx1 pmc1* strain was from Dr. William Wickner (Dartmouth Medical School).⁵⁹ The yeast strain expressing HA-tagged Pmc1-HA was from Dr. Kyle Cunningham (Johns Hopkins University)⁴⁴ and W303-A1 was from Dr. Rodney Rothstein (Columbia University).

4.3 | Vacuole Isolation and in vitro fusion

Vacuoles were isolated as described.⁶⁰ In vitro fusion reactions (30 µL) contained 3 µg each of vacuoles from BJ3505 (*PHO8 pep4*) and DKY6281 (*pho8 PEP4*) backgrounds, reaction buffer 20 mM PIPES-KOH pH 6.8, 200 mM sorbitol, 125 mM KCl, 5 mM MgCl₂, ATP regenerating system (1 mM ATP, 0.1 mg/mL creatine kinase, 29 mM creatine phosphate), 10 µM CoA, and 283 nM Pbi2 (Protease B inhibitor). Fusion was determined by the processing of pro-Pho8 (alkaline phosphatase) from BJ3505 by the Pep4 protease from DK6281. Fusion reactions were incubated at 27°C for 90 minutes and Pho8 activity was measured in 250 mM Tris-HCl pH 8.5, 0.4% Triton X-100, 10 mM MgCl₂, and 1 mM *p*-nitrophenyl phosphate. Pho8 activity was inhibited after 5 minutes by addition of 1 M glycine pH 11 and fusion units were measured by determining the *p*-nitrophenolate produced by detecting absorbance at 400 nm.

4.4 | In vitro Ca²⁺ flux assay

Vacuolar Ca²⁺ flux was measured as described.^{13,16,18} In vitro Ca²⁺ transport reactions (60 µL) contained 20 µg vacuoles from BJ3505 backgrounds, fusion reaction buffer, 10 µM CoA, 283 nM Pbi2 (inhibitor of Proteinase B), and 150 nM of the Ca²⁺ probe Fluo-4 dextran conjugate MW 10000 (Invitrogen) or Cal-520 dextran conjugate MW 10000 (AAT Bioquest). Reaction mixtures were loaded into a black, half-volume 96-well flat-bottom plate with nonbinding surface (Corning). ATP regenerating system or buffer was added, and reactions were incubated at 27°C while Fluo-4 or Cal-520 fluorescence was monitored. Samples were analyzed using a POLARstar Omega fluorescence plate reader (BMG Labtech) with the excitation filter at 485 nm and emission filter at 520 nm for Fluo-4 or Cal-520. Reactions were initiated with the addition of ATP regenerating system following the initial measurement. The effects of inhibitors on efflux were determined by the addition of buffer, inhibitors, or C8-lipids immediately following Ca²⁺ influx. Calibration was done using buffered Ca²⁺ standards (Invitrogen).

4.5 | PI3P 5-kinase assay and thin-layer chromatography

Fab1 kinase activity was measured with an assay adapted from the detection of Fig4 and Plc1 activity^{49,61} with some modifications. Kinase reactions (30 µL) contained 6 µg vacuoles from BJ3505 backgrounds, fusion reaction buffer, ATP regenerating system, 10 µM CoA, 283 nM Pbi2, 2 µM BODIPY-TMR C6-PI3P, and 1 mM sodium orthovanadate. Reaction mixtures were incubated for 1 or 5 minutes at 27°C and then placed on ice. The reactions were immediately quenched with acetone (100 µL). Following incubation acidic phospholipids were extracted from all reactions.⁶² TLC plates (Partisil LK6D Silica Gel Plates [60 Å], Whatman) were pretreated with 1.2 mM EGTA and 1% potassium oxalate (wt/vol) in MeOH/Water (3:2) and then dried at 100°C for 30 minutes prior to use. Dried lipids were resuspended in CHCl₃/MeOH (1:1) (40 µL) and 5 µL was spotted on the plate. Plates were run in CHCl₃/acetone/MeOH/AcOH/Water (46:17:15:14:8). Individual channels were loaded with PI3P and PI(3,5)P₂ standards (Echelon). Imaging of plates was performed using a ChimiDoc MP System (BioRad) and densitometry was determined with Image Lab 4.0.1 software.

4.6 | Vacuole docking

Docking reactions (30 µL) contained 6 µg of wild type vacuoles were incubated in docking buffer (20 mM PIPES-KOH pH 6.8, 200 mM sorbitol, 100 mM KCl, 0.5 mM MgCl₂), ATP regenerating system (0.3 mM ATP, 0.7 mg/mL creatine kinase, 6 mM creatine phosphate), 20 µM CoA, and 283 nM Pbi2.¹⁵ PI(3,5)P₂ was labeled with 2 µM Cy3-GST-ML1-N. Reactions were incubated at 27°C for 20 minutes. After incubating, reaction tubes were placed on ice and vacuoles were stained with 1 µM MDY-64. Reactions were next mixed with 50 µL of 0.6% low-melt agarose (in PS buffer), vortexed to disrupt non-specific clustering, and mounted on slides for observation by fluorescence microscopy. Images were acquired using a Zeiss Axio Observer Z1 inverted microscope equipped with an X-Cite 120XL light source, Plan Aplanachromat 63X oil objective (NA 1.4), and an AxioCam CCD camera.

4.7 | Pmc1-HA immunoprecipitation

Pmc1-HA complex isolation was performed using 20X fusion reactions. Individual reactions were incubated with 150 μ M C8-PI(3,5)P₂, 500 nM GST-ML1-N, 500 μ M Apilimod or buffer alone. After 30 minutes, reactions were placed on ice. Next, reactions were sedimented (11 000g, 10 minutes, 4°C), and the supernatants were discarded before extracting vacuoles with solubilization buffer (SB: 50 mM Tris-HCl, pH 8.0, 2 mM EDTA, 150 mM NaCl, 0.5% Tween-20, 1 mM PMSF). Reactions were then nutated for 1 hour at 4°C. Insoluble debris was sedimented (16 000 g, 10 minutes, 4°C) and 350 μ L of supernatants were removed and placed in chilled tubes. Next, 35 μ L was removed from each reaction as 10% total samples, mixed with 17.5 μ L of 5X SDS loading buffer and 17.5 μ L PS buffer. Equilibrated anti-HA agarose beads (60 μ L) were incubated with the extracts (15 hours, 4°C, nutation). Beads were sedimented and washed 5X with 1 mL SB (800g, 2 minutes, 4°C), and bound material was eluted with 0.1 M Glycine, pH 2.2 and eluates were mixed with SDS-loading buffer. Protein complexes were resolved by SDS-PAGE and examined by Western blotting.

4.8 | Data analysis and statistics

Results are expressed as the mean \pm SEM. Experimental replicates (n) are defined as the number of separate experiments with different vacuole preparations. Significant differences were calculated using unpaired *t* tests. *P* values \leq .05 were considered as significant.

ACKNOWLEDGMENTS

We thank Drs. Kyle Cunningham (Johns Hopkins University), Rodney Rothstein (Columbia University), Lois Weisman (University of Michigan), William Wickner (Dartmouth Medical School) and Haoxing Xu (University of Michigan) for plasmids and yeast strains. This research was supported by grants from the National Institutes of Health (R01-GM101132) and National Science Foundation (MCB 1818310) to RAF.

Funding information

National Institute of General Medical Sciences, Grant/Award Number: GM101132; National Science Foundation, Grant/Award Number: MCB 1818310

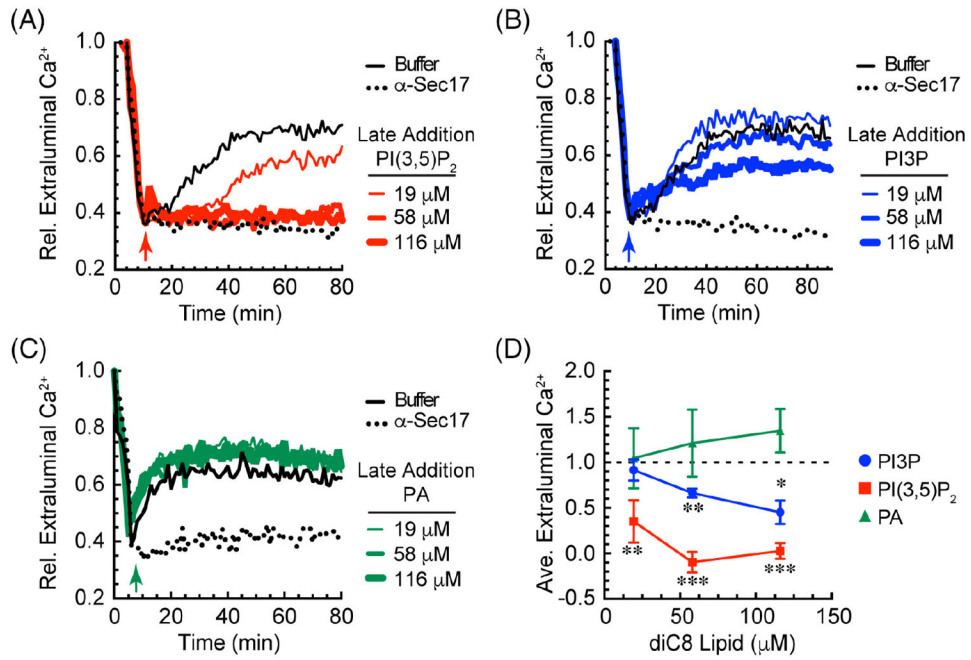
REFERENCES

1. Südhof TC. Calcium control of neurotransmitter release. *Cold Spring Harb Perspect Biol.* 2012;4(1):a011353. [PubMed: 22068972]
2. Chapman ER. How does synaptotagmin trigger neurotransmitter release. *Annu Rev Biochem.* 2008;77:615–641. [PubMed: 18275379]
3. Dunn T, Gable K, Beeler T. Regulation of cellular Ca²⁺ by yeast vacuoles. *J Biol Chem.* 1994;269(10):7273–7278. [PubMed: 8125940]
4. Cunningham KW. Acidic calcium stores of *Saccharomyces cerevisiae*. *Cell Calcium.* 2011;50(2):129–138. [PubMed: 21377728]
5. Bonangelino CJ, Nau JJ, Duex JE, et al. Osmotic stress-induced increase of phosphatidylinositol 3,5-bisphosphate requires Vac14p, an activator of the lipid kinase Fab1p. *J Cell Biol.* 2002;156(6):1015–1028. [PubMed: 11889142]
6. Denis V, Cyert MS. Internal Ca(2+) release in yeast is triggered by hypertonic shock and mediated by a TRP channel homologue. *J Cell Biol.* 2002;156(1):29–34. [PubMed: 11781332]
7. Dong XP, Shen D, Wang X, et al. PI(3,5)P₂ controls membrane trafficking by direct activation of mucolipin Ca(2+) release channels in the endolysosome. *Nat Commun.* 2010;1:38. [PubMed: 20802798]

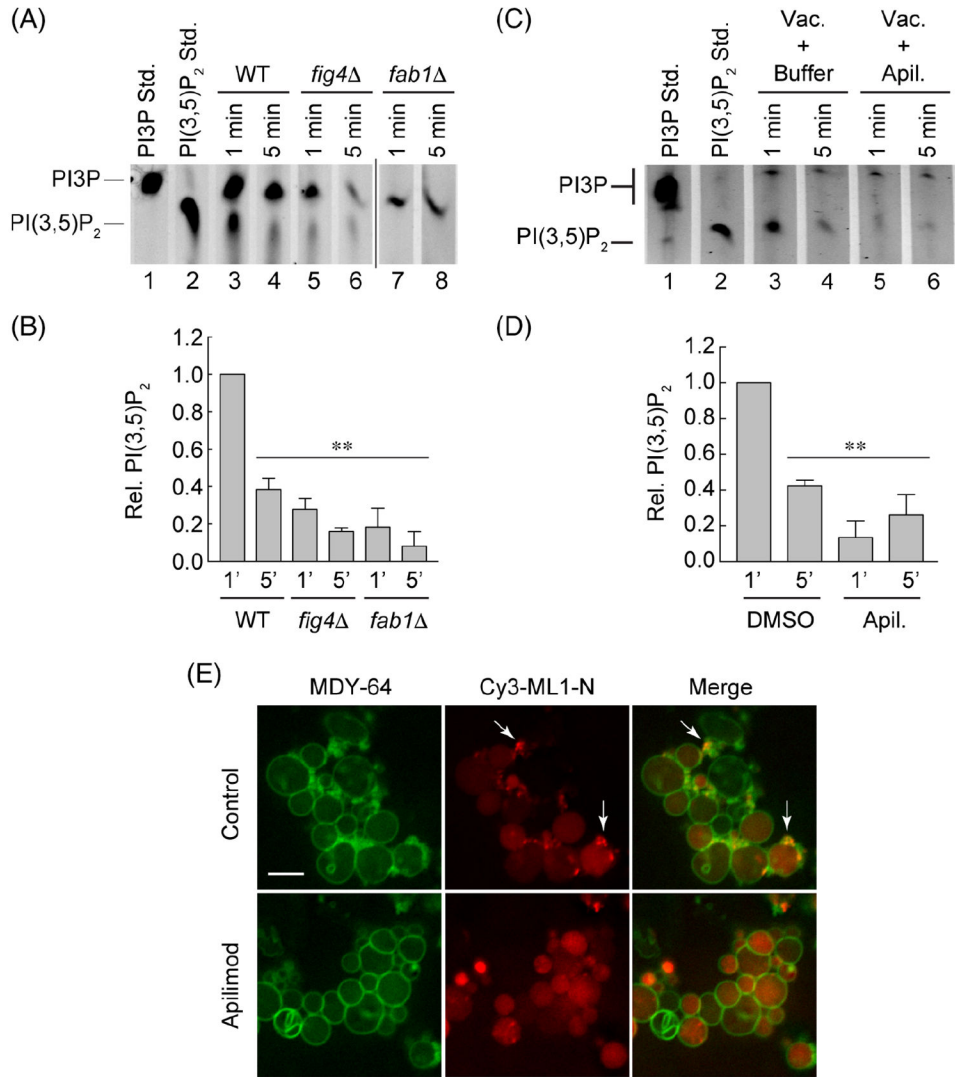
8. Su Z, Anishkin A, Kung C, Saimi Y. The core domain as the force sensor of the yeast mechanosensitive TRP channel. *J Gen Physiol.* 2011; 138(6):627–640. [PubMed: 22124118]
9. Merz AJ, Wickner W. *Trans*-SNARE interactions elicit Ca²⁺ efflux from the yeast vacuole lumen. *J Cell Biol.* 2004;164:195–206. [PubMed: 14734531]
10. Miner GE, Sullivan KD, Guo A, et al. Phosphatidylinositol 3,5-Bisphosphate regulates the transition between trans-SNARE complex formation and vacuole membrane fusion. *Mol Biol Cell.* 2019;30:201–208. [PubMed: 30427760]
11. Ostrowicz CW, Meiringer CT, Ungermann C. Yeast vacuole fusion: a model system for eukaryotic endomembrane dynamics. *Autophagy.* 2008;4(1):5–19. [PubMed: 17932463]
12. Peters C, Mayer A. Ca²⁺/calmodulin signals the completion of docking and triggers a late step of vacuole fusion. *Nature.* 1998;396(6711):575–580. [PubMed: 9859992]
13. Sasser TL, Padolina M, Fratti RA. The yeast vacuolar ABC transporter Ybt1p regulates membrane fusion through Ca²⁺ transport modulation. *Biochem J.* 2012;448(3):365–372. [PubMed: 22970809]
14. Sasser TL, Fratti RA. Class C ABC transporters and vacuole fusion. *Cell Logist.* 2014;4(3):e943588. [PubMed: 25610719]
15. Fratti RA, Jun Y, Merz AJ, Margolis N, Wickner W. Interdependent assembly of specific regulatory lipids and membrane fusion proteins into the vertex ring domain of docked vacuoles. *J Cell Biol.* 2004;167(6):1087–1098. [PubMed: 15611334]
16. Miner GE, Starr ML, Hurst LR, Sparks RP, Padolina M, Fratti RA. The central polybasic region of the soluble SNARE (soluble N-Ethylmaleimide-sensitive factor attachment protein receptor) Vam7 affects binding to phosphatidylinositol 3-phosphate by the PX (Phox homology) domain. *J Biol Chem.* 2016;291(34):17651–17663. [PubMed: 27365394]
17. Miner GE, Starr ML, Hurst LR, Fratti RA. Deleting the DAG kinase Dgk1 augments yeast vacuole fusion through increased Ypt7 activity and altered membrane fluidity. *Traffic.* 2017;18(5):315–329. [PubMed: 28276191]
18. Miner GE, Fratti R. Real-time fluorescence detection of calcium efflux during vacuolar membrane fusion. *Methods Mol Biol.* 1860;2019: 323–331.
19. Mayer A, Wickner W, Haas A. Sec18p (NSF)-driven release of Sec17p (alpha-SNAP) can precede docking and fusion of yeast vacuoles. *Cell.* 1996;85(1):83–94. [PubMed: 8620540]
20. Starr ML, Hurst LR, Fratti RA. Phosphatidic acid sequesters Sec18p from cis-SNARE complexes to inhibit priming. *Traffic.* 2016;17(10):1091–1109. [PubMed: 27364524]
21. Boeddinghaus C, Merz AJ, Laage R, Ungermann C. A cycle of Vam7p release from and PtdIns 3-P-dependent rebinding to the yeast vacuole is required for homotypic vacuole fusion. *J Cell Biol.* 2002;157(1):79–89. [PubMed: 11916982]
22. Karunakaran S, Sasser T, Rajalekshmi S, Fratti RA. Snares, HOPS, and regulatory lipids control the dynamics of vacuolar actin during homotypic fusion. *J Cell Sci.* 2012;14:1683–1692.
23. Karunakaran S, Fratti R. The lipid composition and physical properties of the yeast vacuole affect the hemifusion-fusion transition. *Traffic.* 2013;14(6):650–662. [PubMed: 23438067]
24. Lawrence G, Brown CC, Flood BA, et al. Dynamic association of the PI3P-interacting Mon1-Ccz1 GEF with vacuoles is controlled through its phosphorylation by the type-1 casein kinase Yck3. *Mol Biol Cell.* 2014;25(10):1608–1619. [PubMed: 24623720]
25. Collins MD, Gordon SE. Short-chain phosphoinositide partitioning into plasma membrane models. *Biophys J.* 2013;105(11):2485–2494. [PubMed: 24314079]
26. Mima J, Wickner W. Complex lipid requirements for SNARE- and SNARE chaperone dependent membrane fusion. *J Biol Chem.* 2009;284:27114–27122. [PubMed: 19654322]
27. Cai X, Xu Y, Cheung AK, et al. PIKfyve, a class III PI kinase, is the target of the small molecular IL-12/IL-23 inhibitor apilimod and a player in toll-like receptor signaling. *Chem Biol.* 2013;20(7):912–921. [PubMed: 23890009]
28. Dayam RM, Saric A, Shilliday RE, Botelho RJ. The Phosphoinositide-gated Lysosomal Ca(2+) channel, TRPML1: is required for phagosome maturation. *Traffic.* 2015;16(9):1010–1026. [PubMed: 26010303]

29. Duex JE, Nau JJ, Kauffman EJ, Weisman LS. Phosphoinositide 5-phosphatase Fig 4p is required for both acute rise and subsequent fall in stress-induced phosphatidylinositol 3,5-bisphosphate levels. *Eukaryot Cell*. 2006;5(4):723–731. [PubMed: 16607019]
30. Duex JE, Tang F, Weisman LS. The Vac14p-Fig4p complex acts independently of Vac7p and couples PI3,5P2 synthesis and turnover. *J Cell Biol*. 2006;172(5):693–704. [PubMed: 16492811]
31. Jin N, Chow CY, Liu L, et al. VAC14 nucleates a protein complex essential for the acute interconversion of PI3P and PI(3,5)P(2) in yeast and mouse. *EMBO J*. 2008;27(24):3221–3234. [PubMed: 19037259]
32. Morlock KR, McLaughlin JJ, Lin YP, Carman GM. Phosphatidate phosphatase from *Saccharomyces cerevisiae*. Isolation of 45- and 104-kDa forms of the enzyme that are differentially regulated by inositol. *J Biol Chem*. 1991;266(6):3586–3593. [PubMed: 1995619]
33. Pappu AS, Hauser G. Propranolol-induced inhibition of rat brain cytoplasmic phosphatidate phosphohydrolase. *Neurochem Res*. 1983;8(12):1565–1575. [PubMed: 6324013]
34. Eitzen G, Wang L, Thorngren N, Wickner W. Remodeling of organelle-bound Actin is required for yeast vacuole fusion. *J Cell Biol*. 2002;158(4):669–679. [PubMed: 12177043]
35. Spector I, Shochet NR, Blasberger D, Kashman Y. Latrunculins—novel marine macrolides that disrupt microfilament organization and affect cell growth: I. comparison with cytochalasin D. *Cell Motil Cytoskeleton*. 1989;13(3):127–144. [PubMed: 2776221]
36. Futter CE, Collinson LM, Backer JM, Hopkins CR. Human VPS34 is required for internal vesicle formation within multivesicular endosomes. *J Cell Biol*. 2001;155(7):1251–1264. [PubMed: 11756475]
37. Lang MJ, Strunk BS, Azad N, Petersen JL, Weisman LS. An intramolecular interaction within the lipid kinase Fab1 regulates cellular phosphatidylinositol 3,5-bisphosphate lipid levels. *Mol Biol Cell*. 2017;28(7):858–864. [PubMed: 28148651]
38. Li SC, Diakov TT, Xu T, et al. The signaling lipid PI(3,5)P₂ stabilizes V₁-V(o) sector interactions and activates the V-ATPase. *Mol Biol Cell*. 2014;25(8):1251–1262. [PubMed: 24523285]
39. Starai VJ, Jun Y, Wickner W. Excess vacuolar SNAREs drive lysis and Rab bypass fusion. *Proc Natl Acad Sci U S A*. 2007;104(34):13551–13558. [PubMed: 17699614]
40. Calvert CM, Sanders D. Inositol trisphosphate-dependent and -independent Ca²⁺ mobilization pathways at the vacuolar membrane of *Candida albicans*. *J Biol Chem*. 1995;270(13):7272–7280. [PubMed: 7706267]
41. Teng J, Goto R, Iida K, Kojima I, Iida H. Ion-channel blocker sensitivity of voltage-gated calcium-channel homologue Cch1 in *Saccharomyces cerevisiae*. *Microbiology*. 2008;154(Pt 12):3775–3781. [PubMed: 18803868]
42. Paydar MJ, Pousti A, Farsam H, Amanlou M, Mehr SE, Dehpour AR. Effects of diltiazem or verapamil on calcium uptake and release from chicken skeletal muscle sarcoplasmic reticulum. *Can J Physiol Pharmacol*. 2005;83(11):967–975. [PubMed: 16391705]
43. Takita Y, Engstrom L, Ungermann C, Cunningham KW. Inhibition of the Ca(2+)-ATPase Pmc1p by the v-SNARE protein Nyv1p. *J Biol Chem*. 2001;276(9):6200–6206. [PubMed: 11080502]
44. Cunningham KW, Fink GR. Calcineurin inhibits VCX1-dependent H⁺/Ca²⁺ exchange and induces Ca²⁺ ATPases in *Saccharomyces cerevisiae*. *Mol Cell Biol*. 1996;16(5):2226–2237. [PubMed: 8628289]
45. Tarassov K, Messier V, Landry CR, et al. An in vivo map of the yeast protein interactome. *Science*. 2008;320(5882):1465–1470. [PubMed: 18467557]
46. Fratti RA, Collins KM, Hickey CM, Wickner W. Stringent 3Q: 1R composition of the SNARE 0-layer can be bypassed for fusion by compensatory SNARE mutation or by lipid bilayer modification. *J Biol Chem*. 2007;282(20):14861–14867. [PubMed: 17400548]
47. Bayer MJ, Reese C, Buhler S, Peters C, Mayer A. Vacuole membrane fusion: V0 functions after trans-SNARE pairing and is coupled to the Ca²⁺-releasing channel. *J Cell Biol*. 2003;162(2):211–222. [PubMed: 12876274]
48. Sasser T, Qiu QS, Karunakaran S, et al. Yeast lipin 1 orthologue pah1p regulates vacuole homeostasis and membrane fusion. *J Biol Chem*. 2012;287(3):2221–2236. [PubMed: 22121197]

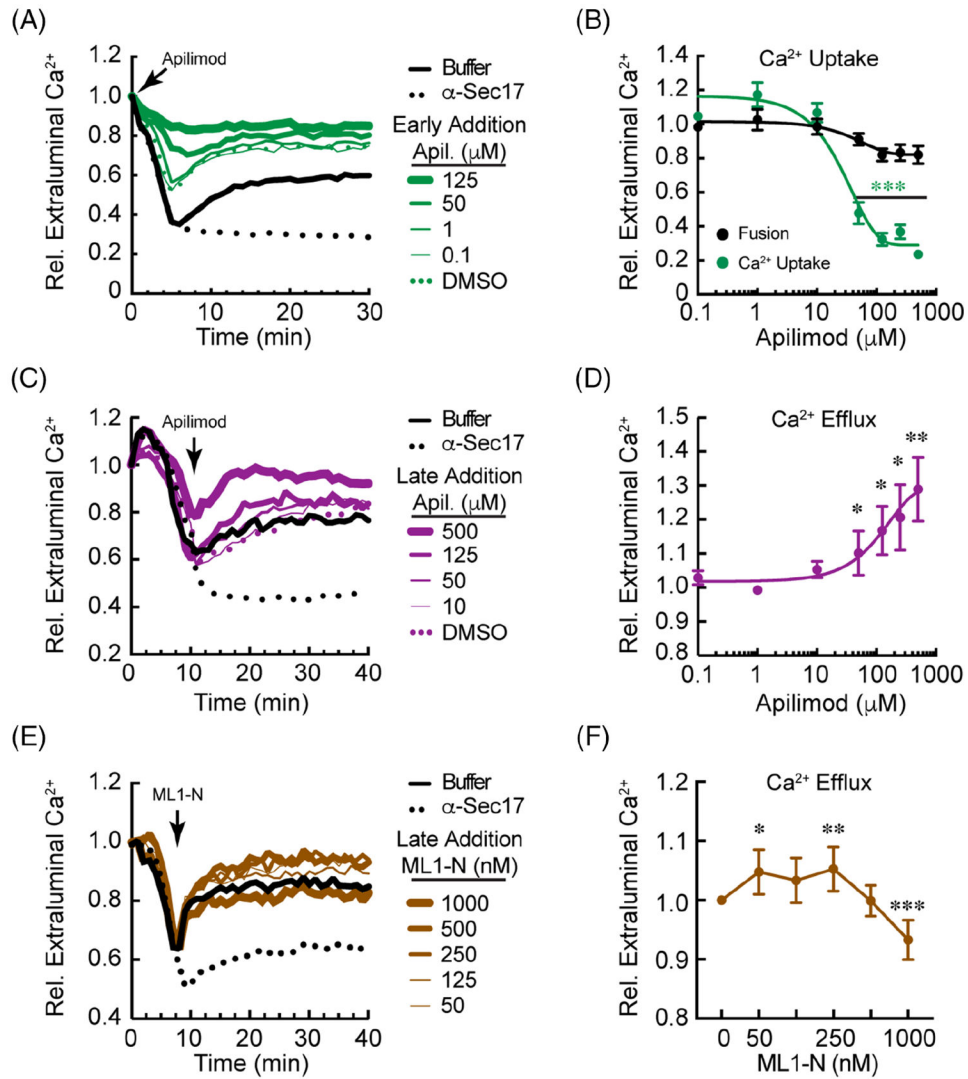
49. Jun Y, Fratti RA, Wickner W. Diacylglycerol and its formation by phospholipase C regulate Rab- and SNARE-dependent yeast vacuole fusion. *J Biol Chem*. 2004;279:53186–53195. [PubMed: 15485855]
50. Mayer A, Scheglmann D, Dove S, Glatz A, Wickner W, Haas A. Phosphatidylinositol 4,5-bisphosphate regulates two steps of homotypic vacuole fusion. *Mol Biol Cell*. 2000;11(3):807–817. [PubMed: 10712501]
51. Banerjee S, Clapp K, Tarsio M, Kane PM. Interaction of the late endolysosomal lipid PI(3,5)P₂ with the Vph1 isoform of yeast V-ATPase increases its activity and cellular stress tolerance. *J Biol Chem*. 2019;294:9161–9171. [PubMed: 31023825]
52. Di Giovanni J, Boudkazi S, Mochida S, et al. V-ATPase membrane sector associates with synaptobrevin to modulate neurotransmitter release. *Neuron*. 2010;67(2):268–279. [PubMed: 20670834]
53. Miseta A, Kellermayer R, Aiello DP, Fu L, Bedwell DM. The vacuolar Ca²⁺/H⁺ exchanger Vcx1p/Hum1p tightly controls cytosolic Ca²⁺ levels in *S. cerevisiae*. *FEBS Lett*. 1999;451(2):132–136. [PubMed: 10371152]
54. Chandel A, Das KK, Bachhawat AK. Glutathione depletion activates the yeast vacuolar transient receptor potential channel, Yvc1p, by reversible glutathionylation of specific cysteines. *Mol Biol Cell*. 2016;27(24):3913–3925. [PubMed: 27708136]
55. Hamamoto S, Mori Y, Yabe I, Uozumi N. In vitro and in vivo characterization of modulation of the vacuolar cation channel TRPY1 from *Saccharomyces cerevisiae*. *FEBS J*. 2018;285(6):1146–1161. [PubMed: 29405580]
56. Schlecht U, Miranda M, Suresh S, Davis RW, St Onge RP. Multiplex assay for condition-dependent changes in protein-protein interactions. *Proc Natl Acad Sci U S A*. 2012;109(23):9213–9218. [PubMed: 22615397]
57. Li SC, Diakov TT, Rizzo JM, Kane PM. Vacuolar H⁺-ATPase works in parallel with the HOG pathway to adapt *Saccharomyces cerevisiae* cells to osmotic stress. *Eukaryot Cell*. 2012;11(3):282–291. [PubMed: 22210831]
58. Slusarewicz P, Xu Z, Seefeld K, Haas A, Wickner WT. I2B is a small cytosolic protein that participates in vacuole fusion. *Proc Natl Acad Sci U S A*. 1997;94(11):5582–5587. [PubMed: 9159115]
59. Ungermann C, Wickner W, Xu Z. Vacuole acidification is required for trans-SNARE pairing, LMA1 release, and homotypic fusion. *Proc Natl Acad Sci U S A*. 1999;96(20):11194–11199. [PubMed: 10500153]
60. Haas A, Conradt B, Wickner W. G-protein ligands inhibit in vitro reactions of vacuole inheritance. *J Cell Biol*. 1994;126(1):87–97. [PubMed: 8027189]
61. Rudge SA, Anderson DM, Emr SD. Vacuole size control: regulation of PtdIns(3,5)P₂ levels by the vacuole-associated Vac14-Fig4 complex, a PtdIns(3,5)P₂-specific phosphatase. *Mol Biol Cell*. 2004;15(1):24–36. [PubMed: 14528018]
62. Sasser TL, Lawrence G, Karunakaran S, Brown C, Fratti RA. The yeast ABC transporter Ycf1p enhances the recruitment of the soluble SNARE Vam7p to vacuoles for efficient membrane fusion. *J Biol Chem*. 2013;288:18300–18310. [PubMed: 23658021]
63. Jones EW, Zubenko GS, Parker RR. PEP4 gene function is required for expression of several vacuolar hydrolases in *Saccharomyces cerevisiae*. *Genetics*. 1982;102(4):665–677. [PubMed: 6764901]
64. Wallis JW, Chrebet G, Brodsky G, Rolfe M, Rothstein R. A hyper-recombination mutation in *S. cerevisiae* identifies a novel eukaryotic topoisomerase. *Cell*. 1989;58(2):409–419. [PubMed: 2546682]

**FIGURE 1.**

PI(3,5)P₂ blocks Ca^{2+} efflux from vacuoles during fusion. Vacuoles were harvested from BJ3505 and 2X fusion reactions containing 150 μ M Fluo-4 dextran. After 10 minutes of incubation with ATP (arrow) at 27°C to allow for the uptake of Ca^{2+} , reactions were incubated with C8-PI(3,5)P₂ (A), C8-PI3P (B) or C8-PA (C) at the indicated concentrations. Reactions were further incubated at 27°C and fluorescence was measured every 30 seconds for 80 minutes. Values were normalized to 1.0 representing the extraluminal Ca^{2+} at the beginning of the reaction and expressed as relative (Rel.) values compared to the untreated control. Separate reactions were incubated with 140 μ g/mL anti-Sec17 IgG to block SNARE-dependent Ca^{2+} efflux. D, Average Ca^{2+} efflux from A to C. The maximum efflux for the untreated control was normalized to 1 and the results from the treatments were calculated in relation to the untreated control. Error bars are SEM (n = 3). Significant differences were in comparison the untreated control (buffer) * P < .05, ** P < .01, *** P < .001 (Unpaired t test)

**FIGURE 2.**

Apilimod inhibits Fab1 activity. A, Vacuoles were incubated with BODIPY-TMR C6-PI3P at 27°C after which reactions were quenched with acetone and lipids were extracted and resolved by TLC to detect the production of BODIPY-TMR C6-PI(3,5)P₂ by Fab1 activity. Wild type vacuoles were tested in parallel to those from *fig4* and *fab1* strains. Pure BODIPY-TMR C6-PI3P and C6-PI(3,5)P₂ were used as standards in lanes 1 and 2. B, Average of three experiments in panel A. C, Vacuoles were incubated with DMSO (carrier) or 500 μM Apilimod. D, Average of three experiments in panel C. E, Vacuoles were incubated under docking conditions for 20 minutes. Endogenous PI(3,5)P₂ was labeled with 2.5 μM Cy3-ML1-N and the total membranes were labeled with 1 μM MDY-64. Vacuoles were incubated with Apilimod or DMSO. Arrows point at examples of PI(3,5)P₂ puncta. Error bars are SEM (n = 3). Significant differences were in comparison wild type or DMSO at 1 minute ***P* < .01 (unpaired *t* test). Scale bar: 2 μm

**FIGURE 3.**

Apilimod modulates Ca^{2+} flux during vacuole fusion. A, Vacuoles were incubated with buffer, 140 $\mu\text{g}/\text{mL}$ anti-Sec17 IgG, Apilimod or DMSO (Carrier) at the beginning of the reaction and incubated for 30 minutes to monitor Ca^{2+} flux. B, Quantitation of Ca^{2+} efflux at 30 minutes normalized to the untreated control. In parallel, vacuole fusion was measured in the presence of Apilimod. The maximum Ca^{2+} efflux for the untreated control was normalized to 1 and the results from the treatments were calculated in relation to the untreated control. C, Vacuoles were incubated with buffer or 140 $\mu\text{g}/\text{mL}$ anti-Sec17 IgG and incubated for 8 to 10 minutes to allow Ca^{2+} uptake. Next, vacuoles were incubated with a concentration range of Apilimod or DMSO (Carrier). Reactions were further incubated for a total 40 minutes. D, Quantitation of Ca^{2+} efflux at 30 minutes normalized to the untreated control. Results were normalized as in described in B. E, Vacuoles were incubated with buffer or anti-Sec17 IgG and incubated for 10 minutes to allow Ca^{2+} uptake. Next, vacuoles were incubated with a concentration range of GST-ML1-N and reactions were further incubated for a total of 30 minutes. F, Ca^{2+} release at 30 minutes. Results were

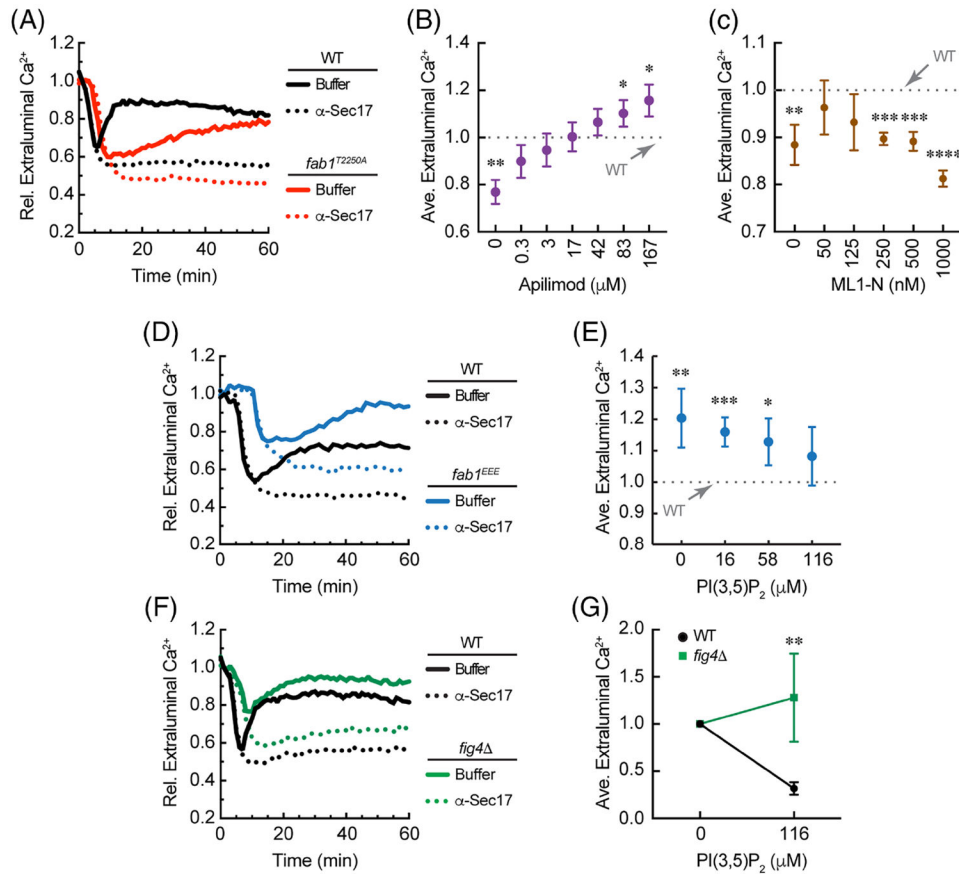
normalized as in described in B. Error bars are SEM (n = 3). * $P < .05$, ** $P < .01$, *** $P < .001$ (unpaired t test). Significant differences were in comparison to untreated wild type efflux

Author Manuscript

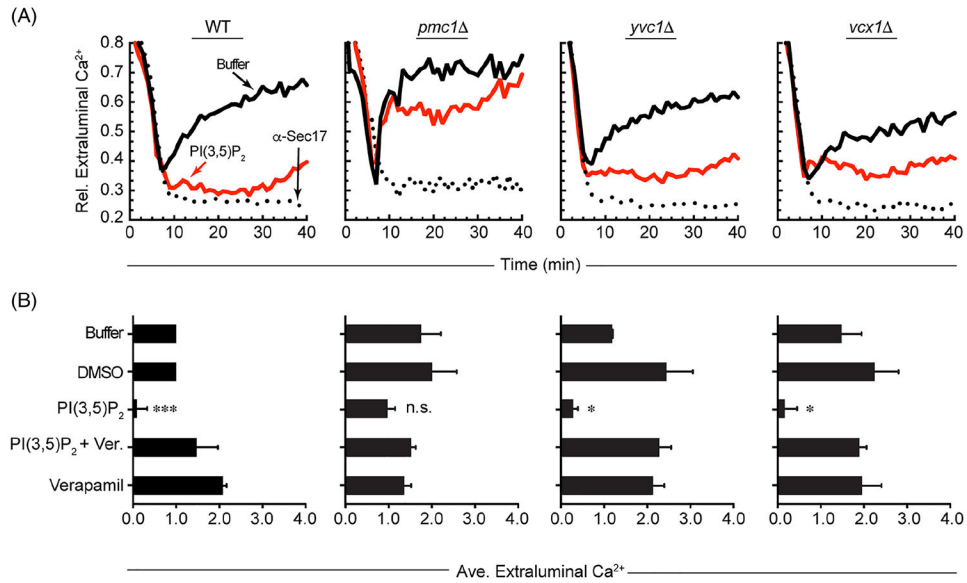
Author Manuscript

Author Manuscript

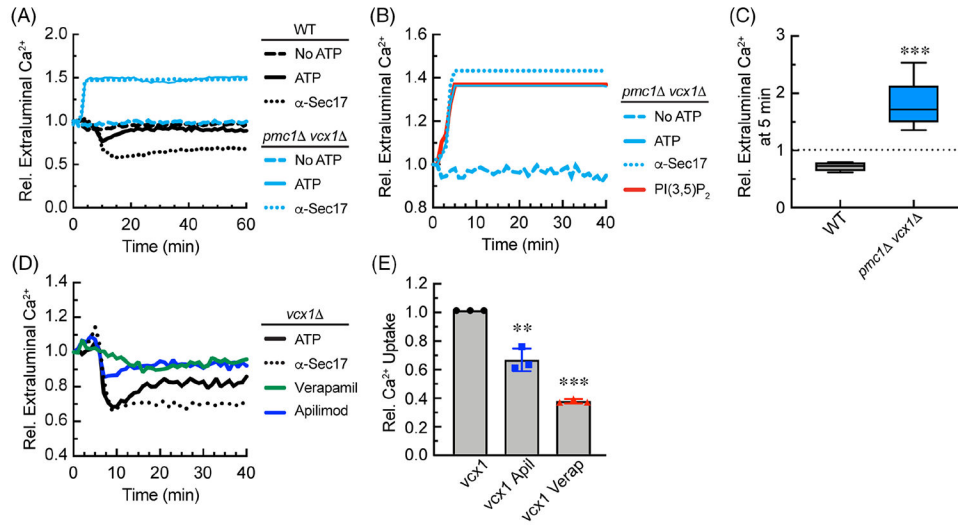
Author Manuscript

**FIGURE 4.**

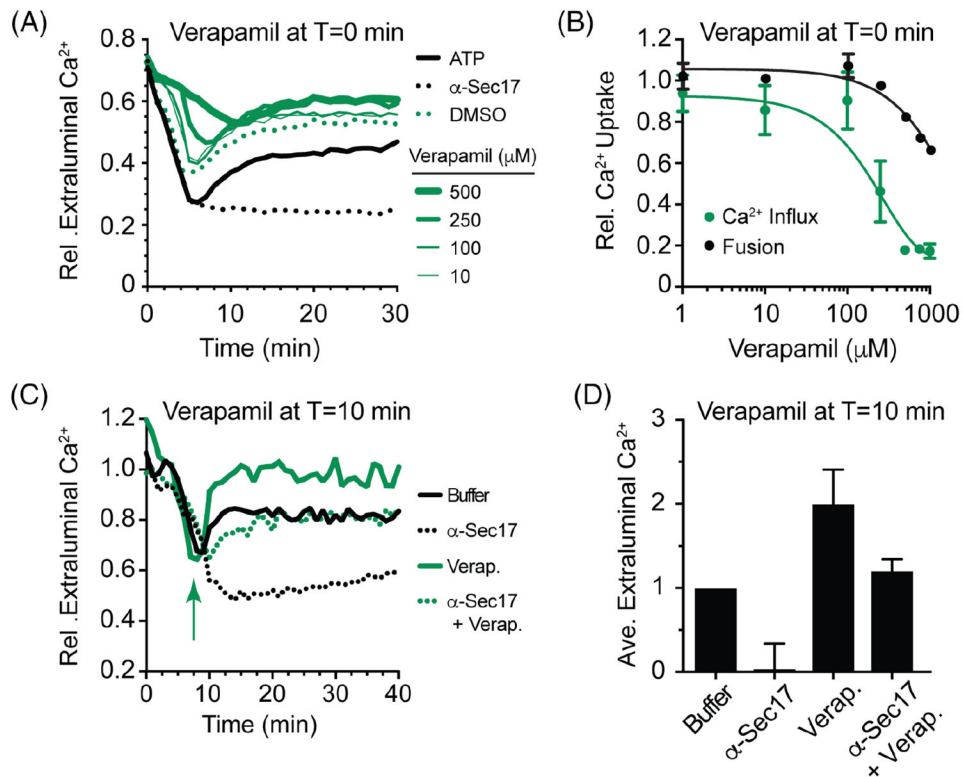
FAB1 kinase mutations differentially affect Ca^{2+} transport. Vacuoles from wild type yeast were tested for Ca^{2+} transport in parallel with those from *fab1*^{T2250A} (A), *fab1*^{EEE} (D) or *fig4* (F) yeast. B, *Fab1*^{T2250A} vacuoles were incubated with a concentration range of Apilimod after 10 minutes of incubation. Reactions were then incubated for a total of 60 minutes. Average Ca^{2+} efflux values at 30 minutes of incubation were normalized relative to wild type given a value of 1 (dotted line). C, *Fab1*^{T2250A} vacuoles were incubated with a concentration range of GST-ML1-N as done with Apilimod. Values were normalized to wild type efflux at 30 minutes. D, *fab1*^{EEE} vacuoles were incubated with a dose curve of C8-PI(3,5)P₂ and incubated in parallel with wild type vacuoles. Values were taken at 30 minutes and normalized wild type efflux without treatment at 30 minutes. E, Quantitation of *fab1*^{EEE} vacuole flux in the presence of C8-PI(3,5)P₂. Values were normalized to wild type efflux, which was set to 1. F, Wild type vacuoles were incubated in parallel with and *fig4* vacuoles incubated with buffer or C8-PI(3,5)P₂. Efflux values were taken at 30 minutes with or without treatment for wild type and *fig4* vacuoles. G, Comparison of the maximal effects of C8-PI(3,5)P₂ on Ca^{2+} flux between wild type and *fig4* vacuoles. Values were normalized to the no treatment condition for each vacuole type. Error bars are SEM (n = 3). Significant differences were in comparison wild type. * $P < .05$, ** $P < .01$, *** $P < .001$, **** $P < .0001$ (unpaired *t* test)

**FIGURE 5.**

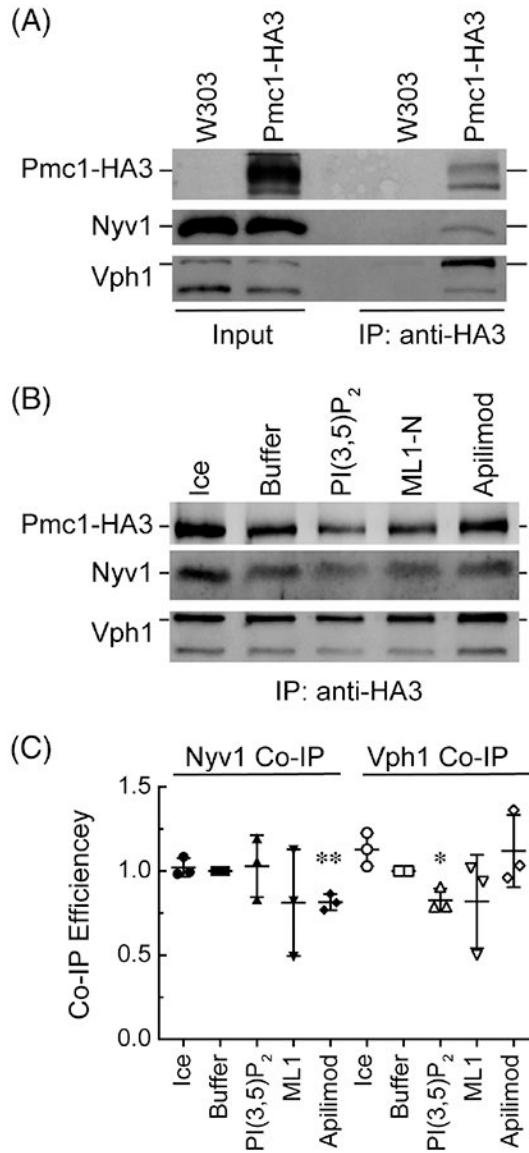
PI(3,5)P₂ regulates Ca²⁺ transport through Pmc1 during fusion. A, Vacuoles isolated from wild type as well as *pmc1*, *yvc1* and *vcx1* strains were used in Ca²⁺ transport assays as described. Reactions were incubated with 140 μg/mL anti-Sec17, buffer or 116 μM C8-PI(3,5)P₂ added after 5 minutes of incubation. Reactions were incubated for a total of 40 minutes and fluorescence was measured every 60 seconds. B, Average Ca²⁺ transport levels for multiple experiments with wild type, *pmc1*, *yvc1* or *vcx1* vacuoles. After 10 minutes of incubation reactions were incubated with buffer, DMSO, 116 μM C8-PI(3,5)P₂, 500 μM Verapamil or C8-PI(3,5)P₂ and Verapamil together and incubated for a total of 40 minutes. The extraluminal Ca²⁺ at the end of 40 minutes was normalized to 1 for the buffer and DMSO controls. The amount of extraluminal Ca²⁺ for each treatment was then normalized to the controls. Error bars are SEM (n = 3). Significant differences were in comparison the untreated control (buffer) **P* < .05, ****P* < .001 (unpaired *t* test)

**FIGURE 6.**

Vacuoles lacking both Pmc1 and Vcx1 expel Ca²⁺ in an ATP-dependent manner. A, Compares the Ca²⁺ transport profiles of wild type vs the *pmc1 vcx1* double deletion vacuoles. Individual reactions were in the presence of reaction buffer alone, buffer with ATP, or buffer with ATP and 140 μg/mL anti-Sec17 IgG. B, Effect of C8-PI(3,5)P₂ on Ca²⁺ flux by *pmc1 vcx1* double deletion vacuoles. C, Quantitation of relative Ca²⁺ flux into or out of vacuole from wild type and *pmc1 vcx1* double deletion yeast after 5 minutes of incubation. The extraluminal Ca²⁺ in the absence of ATP was set to 1 and the results in the presence of ATP were normalized to the no ATP control. D, Vacuoles from *vcx1* yeast were incubated with 140 μg/mL anti-Sec17 IgG, 500 μM Verapamil or 125 μM Apilimod added at *T* = 0 min. E, Quantitation of relative Ca²⁺ uptake wild type and *vcx1* vacuoles after 10 minutes of incubation. The extraluminal Ca²⁺ in the untreated control was set to 1 and the results with Apilimod and Verapamil was normalized to the untreated control. Error bars are SEM (n = 3). Significant differences were in comparison the untreated control (buffer) ***P* < .01, ****P* < .001 (unpaired *t* test)

**FIGURE 7.**

Verapamil inhibits Ca^{2+} uptake. A, Wild type vacuoles were incubated with a dose curve of Verapamil at $T = 0$ minute to block Ca^{2+} uptake. Separate reactions were incubated with buffer, DMSO or anti-Sec17 as controls. Reactions were incubated for a total of 30 minutes and fluorescence was measured every 30 seconds. B, Average Ca^{2+} transport levels for multiple experiments shown in panel A (green). The extraluminal Ca^{2+} for the untreated control after 5 minutes of incubation was normalized to 1. The result for each concentration of Verapamil was normalized as a fraction of the untreated control. In parallel, the effects of Verapamil on vacuole fusion (black). C, Wild type vacuoles were incubated with 500 μM Verapamil or DMSO after 8 minutes of incubation to allow initial Ca^{2+} uptake. Reactions were analyzed as described in panel A. D, Average Ca^{2+} transport levels for multiple experiments shown in panel C. The changes were determined by taking the difference between maximum uptake and efflux signals for each condition and normalized relative to control (buffer) conditions set to 1

**FIGURE 8.**

The effects of PI(3,5)P₂ levels on Pmc1 interactions. A, Vacuoles from wild type yeast and a strain expressing HA-tagged Pmc1 were compared by immunoprecipitation with anti-HA beads and immunoblotting for isolated complexes. B, Vacuoles expressing Pmc1-HA3 were incubated in large scale reactions (20X) in the presence of 150 μM C8-PI(3,5)P₂, 500 nM ML1-N, 500 μM Apilimod or buffer alone. Reactions were incubated for 30 minutes at 27°C. After incubating, the reactions were placed on ice and solubilized and processed for immunoprecipitation with anti-HA agarose. Protein complexes were eluted with sodium thiocyanate and resolved by SDS-PAGE and probed by Western blotting for the presence of Pmc1-HA3 and Nyv1. C, Average quantitation of Nyv1 and Vph1 bound to Pmc1-HA. Western blot band intensities were measured using ImageJ (NIH). Values for the buffer control at 27°C were set to 1 and the other values were normalized relative to this control. Values represent concentrations relative to Pmc1-HA3 at $T = 30$ minutes. Error

bars represent SD (n = 3). Significant differences were in comparison to the buffer control at 27°C * $P < .05$, ** $P < .01$ (unpaired t test)

Author Manuscript

Author Manuscript

Author Manuscript

Author Manuscript

TABLE 1

Yeast strains used in this study

Strain	Genotype	Source
BJ3505	<i>MATα ura3-52 trp1- 101 his3-200 lys2-801 gal2 (gal3) can1 prb1- 1.6R pep4::HIS3</i>	63
DKY6281	<i>MATα pho8::TRP1 leu2-3 leu 2-112 ura3-52 his3-200 trp1- 901 lys2-801</i>	60
W303-1A	<i>MATα leu2-3112 trp1-1 ura3-1 his3-11 can1-100</i>	64
K699	W303-1A, <i>PMC1::3XHA</i>	44
<i>vcx1 pmc1</i>	BJ3505, <i>vcx1::URA3 pmc1::TRP1</i>	59
RFY74	BJ3505, <i>yvc1::kanMX6</i>	10
RFY76	BJ3505, <i>fab1::kanMX6</i>	10
RFY78	RFY76, <i>pRS416-FAB1^{T2250A}</i>	10
RFY80	RFY76, <i>pRS416-FAB1^{EEE}</i>	10
RFY82	BJ3505, <i>fig4::kanMX6</i>	10
RFY84	BJ3505, <i>pmc1::kanMX6</i>	This study
RFY86	BJ3505, <i>vcx1::kanMX6</i>	This study